Supplementary information

Stabilization of COOH* intermediate through hydroxylation engineering for remarkably efficient photocatalytic CO_2 reduction

Zhende Wu, Jing Xie*, Zhenjiang Lu, Jindou Hu, Yali Cao*

State Key Laboratory of Chemistry and Utilization of Carbon Based Energy Resources, College of Chemistry, Xinjiang University, Urumqi, 830046, Xinjiang, PR China.

*Corresponding author. Tel: +86-991-8583083; Fax: +86-991-8588883; Email: caoyali523@163.com (Y. Cao); xiejing@xju.edu.cn (J. Xie).

1. Experimental section

1.1. Chemicals

Titanium oxide sulfate ($TiOSO_4 \cdot xH_2SO_4 \cdot xH_2O$, Aladdin Reagent Shanghai Co., Ltd.), strontium nitrate ($Sr(NO_3)_2$, Aladdin Reagent Shanghai Co., Ltd.) and sodium hydroxide (NaOH, Tianjin Xinbote Chemical Co., Ltd.) were all commercially available analytically pure reagents in the experiment.

1.2. Synthesis of oxygen-rich vacancy $SrTiO_3$

Oxygen-rich vacancy $SrTiO_3$ was synthesized via a low-heating solid-state precursor method. A mixture of 10 mmol of $TiOSO_4$ and 40 mmol of NaOH was subjected to agate mortar to form a homogeneous powder, which was sustained for a duration of 30 min to ensure complete reaction between the two reagents. Subsequently, the reaction system was supplemented with 4 mmol of $Sr(NO_3)_2$, and the solid reaction process was continued for an additional period of approximately 30 min to facilitate the formation of the precursor material. The mixture was then subjected to calcination under an air atmosphere at a heating rate of 5°C per minute for a duration of 5 h at temperature of 700°C. Following calcination, the resulting brownish-gray solid was washed consecutively three times using deionized water and ethanol solutions to remove any unreacted precursors or byproducts. Eventually, the product is dried overnight in a vacuum oven at 80°C and the final product is labeled as STO.

1.3 Synthesis of Hydroxyl modified STO

A total of 1.1 mmol of STO was added to 60 mL of NaOH solution at a concentration of 5 M. The mixture was stirred for 10 min and subsequently transferred to a 100 mL reactor. The reactor was subjected to hydrothermal treatment at 140°C for varying durations of 1, 3, 5, 7, and 9 h, respectively. After the treatment, the products were collected and washed three times alternately with water and ethanol, followed by drying overnight in a vacuum oven at 80°C. The resulting products were designated as

STO-OH-1, STO-OH-3, STO-OH-5, STO-OH-7, and STO-OH-9, corresponding to the different hydrothermal reaction times.

The concentration of the alkaline solution was changed to 0, 1, and 9M while other procedural steps unchanged, and designate the products as STO-C0M, STO-C1M, and STO-C9M.

1.4. Characterization of photocatalysis

The crystallographic information of samples was investigated by performing X-ray powder diffraction (XRD) characterization using a D8 Advance X-ray diffractometer with non-monochromated Cu Kα X-ray source (λ=1.054056 Å) in an operating voltage of 40 kV and a beam current of 40 mA. The morphology was observed by field emission scanning electron microscopy (FESEM, Hitachi S-4800H) using an accelerating voltage of 5 kV, transmission electron microscopy (TEM, Hitachi H-600) using an accelerating voltage of 120 kV, and high-resolution transmission electron microscopy (HR-TEM, JEOL JEM-2010F) using an accelerating voltage of 200 kV. The element component was measured by the energy disperse X-ray spectrum (EDS, EDAXTLS). X-ray photoelectron spectroscopy (XPS) (Thermo Fisher Scientific ESCALAB250Xi) employing Al Kα (1486.6 eV) was taken to identify the surface components and valence states of products. Oxygen vacancy was measured on electron paramagnetic resonance (EPR) spectrometer (MEX-nano, Bruker). The optical properties and energy band structure of the samples were tested by UV-vis Diffuse Reflectance Spectroscopy (UV-vis, DRS). Fourier transform infrared (FT-IR) spectra of the generated samples are recorded with a Bruker VERTEX 70 spectrometer in the range 4000 to 400 cm^{-1} using the KBr method. Steady-state and time resolved photolumminescence spectra (PL, Hitachi F-4500) was used to determine the fluorescence intensity of the sample and analyze the complex separation efficiency of photogenerated carriers. The fluorescence lifetime of the sample was determined using a transient fluorescence spectrometer (TRPL, Fluorolog-3). The appropriate excitation wavelength was set according to the temperature-programmed desorption of CO_2 (CO_2-TPD, Thremo TPDRO 1100). A combined analysis employing thermogravimetric

analysis (TGA), in-situ Fourier transform infrared spectroscopy (FTIR), and mass spectrometry (MS) was performed to study of catalyst surface information. The surface charge distribution of the sample was determined using a nanosizer and zeta potential analyzer (Zeta, Nano ZS90).

Photoelectrochemical measurements were conducted using a three-electrode system on an electrochemical workstation (CHI760E). In this setup, a platinum net served as the counter electrode, an Ag/AgCl electrode functioned as the reference electrode, and the working electrode comprised indium tin oxide (ITO) glass coated with photocatalysts. To prepare the working electrode, 1 mg of the catalyst was dispersed in 1 mL of ethanol and 20 μL of Nafion. This mixture was sonicated for 30 minutes before being deposited onto the surface of the conductive glass (with an area of 2 cm^2) and dried overnight at 80°C to form a thin film. A sodium sulfate (Na_2SO_4) solution at a concentration of 0.5 $mol \cdot L^{-1}$ was used as the electrolyte. For transient photocurrent (I-t) measurements, the light was switched on and off every 30 seconds, with excitation provided by a 300 W xenon lamp (model PLS-SXE300D). Mott-Schottky experiments were performed at a frequency of 2000 Hz, while electrochemical impedance spectroscopy (EIS) was conducted over a frequency range of 0.1 to 100000 Hz.

S4. Photocatalysis performances measurements

In this study, the activity of the photocatalysts was evaluated using a LabSolar-6A photochemical reactor equipped with a sealed glass photocatalytic reactor. The experimental procedure is outlined as follows: First, 0.5 mL of triethanolamine was dissolved in 4.5 mL of deionized water, followed by the addition of 10 mg of the photocatalyst. The mixture was then subjected to ultrasonic treatment for 10 min. Subsequently, the resulting suspension was transferred to a 200 mL airtight quartz photocatalytic reactor. Temperature of the reactor was controlled at 5°C by a circulating water-cooling system. Before illumination, the reaction system was first vacuated and slowly pumped with high purity CO_2 (99.99%) until the pressure became steady at 80 MPa. The above operation was repeated three times to exhaust air from the reaction

system thoroughly. After stirring for 30 min, the adsorption-desorption balance between the photocatalyst and CO_2 could be established. The intermediate products for CO_2 adsorption and reduction were analyzed from in-situ Fourier transform infrared spectroscopy (in-situ FTIR, Bruker INVENIO R).

During the photocatalytic reaction, a 300 W xenon lamp (model PLS-SXE300D) was utilized as the light source. An online gas chromatography system, equipped with a thermal conductivity detector (TCD) and a flame ionization detector (FID), was used to analyze the gaseous products every 0.5 h. Notably, the detection of carbon-containing products was conducted using the FID. Argon served as the carrier gas throughout the photocatalytic reaction, which lasted for a total of 2.5 h. By analyzing the peak positions and areas in the chromatograms, the types and yields of the products resulting from photocatalytic CO_2 conversion were determined.

Supplementary Figs and Tables

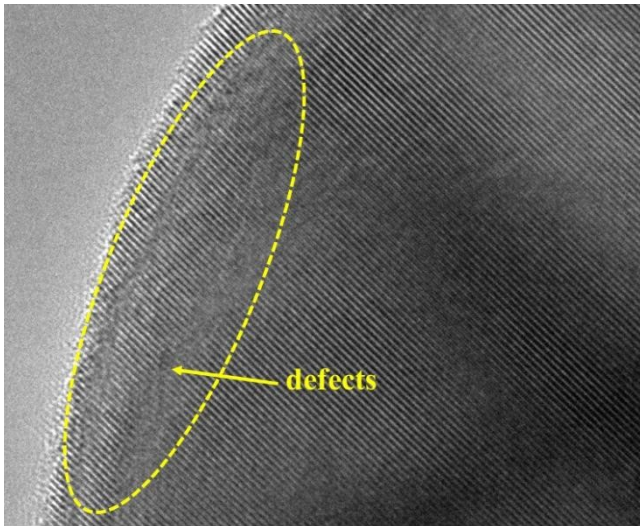

Fig. S1 HRTEM images of STO-OH-5.

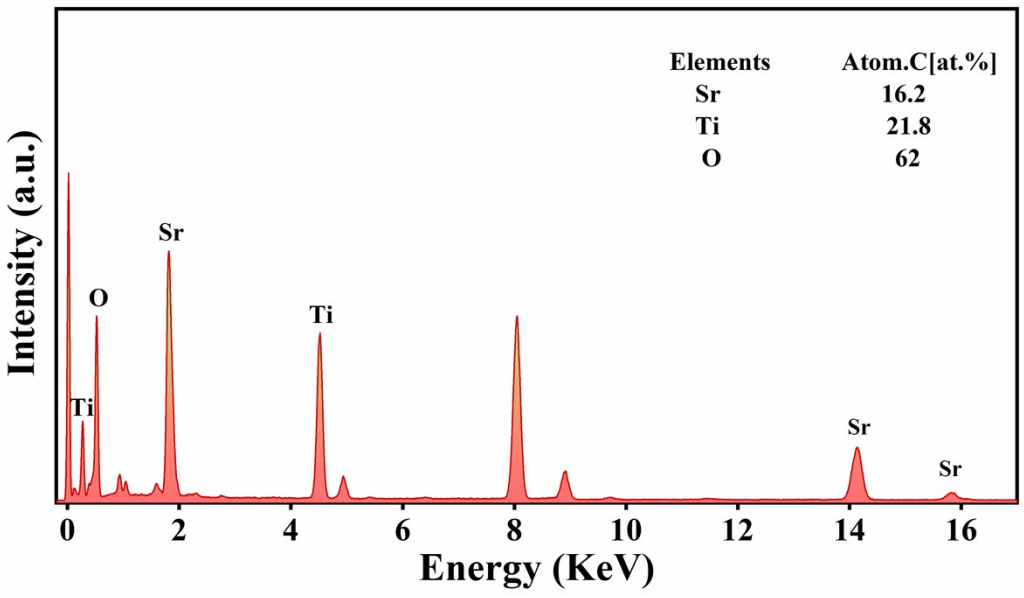

Fig. S2 EDS spectrum of STO-OH-5 sample.

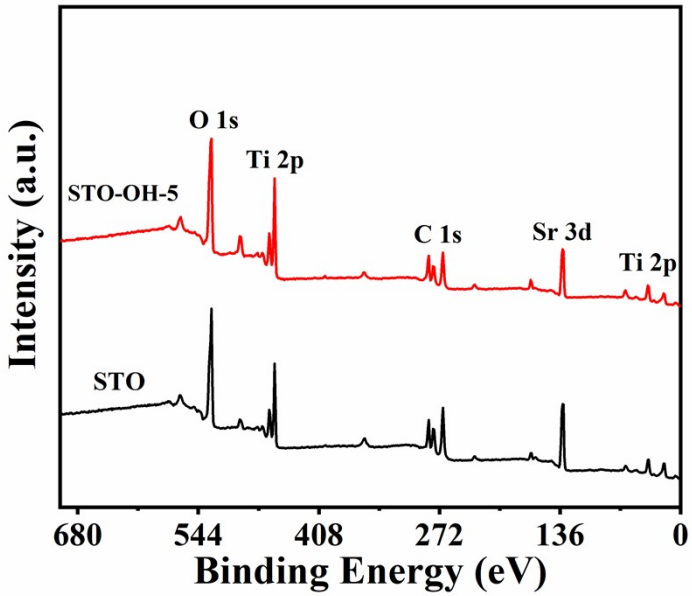

Fig. S3 XPS survey spectra of STO and STO-OH-5.

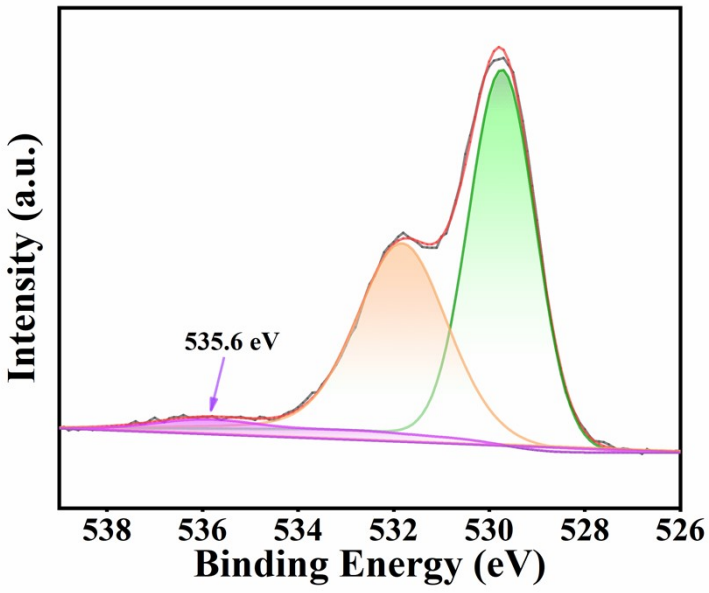

Fig. S4 XPS O1s spectra of STO-OH-5.

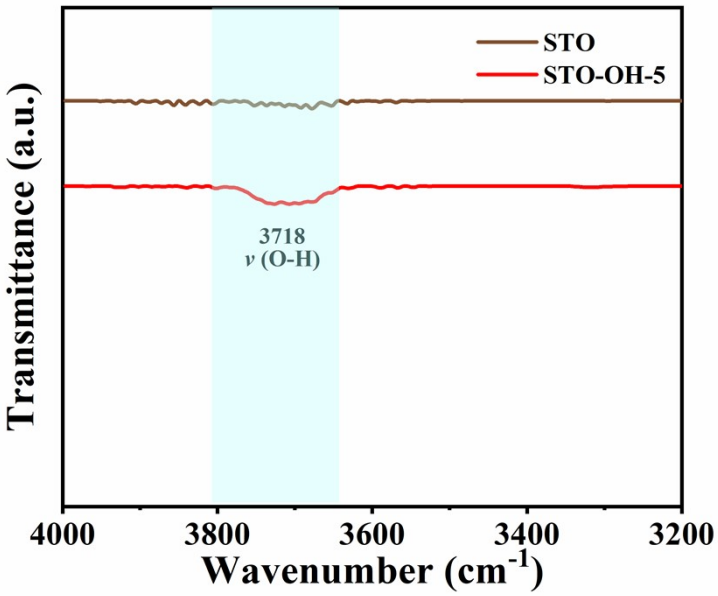

Fig. S5 Local amplified FT-IR spectra of STO and STO-OH-5.

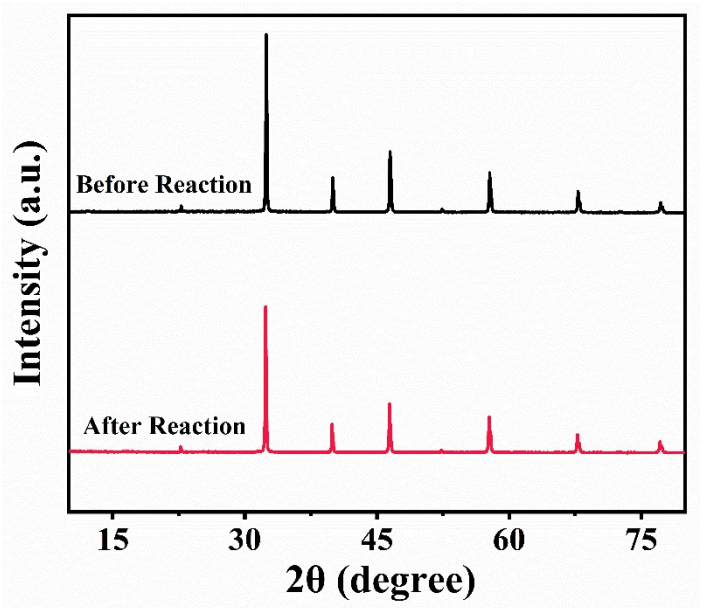

Fig. S6 The XRD of the cycled STO-OH-5.

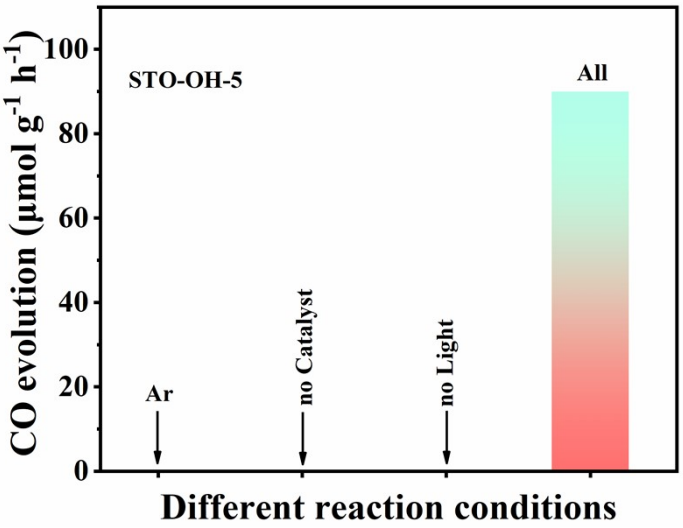

Fig. S7 Photocatalytic CO_2 reduction experiments under various reaction conditions.

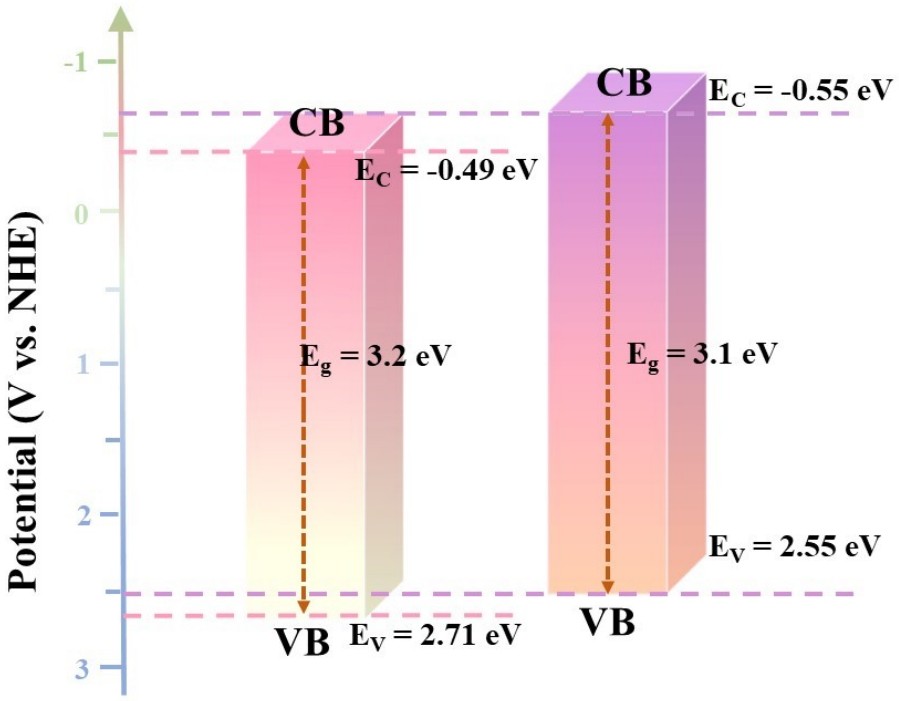

Fig. S8 The energy band structures of STO and STO-OH-5.

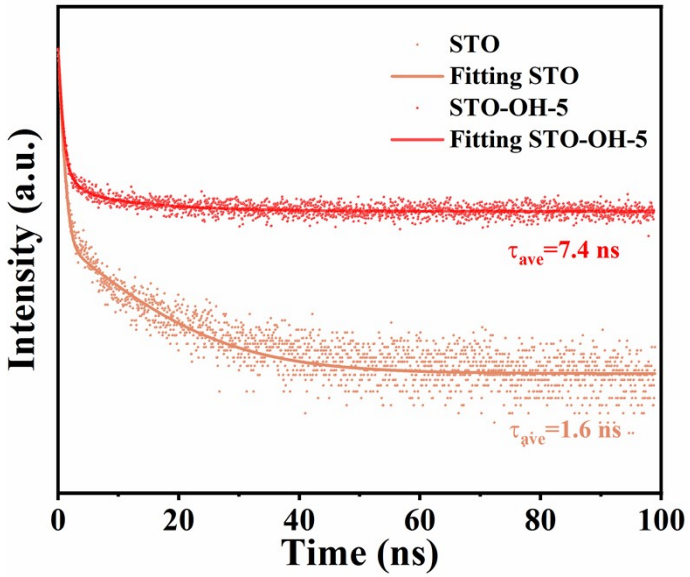

Fig. S9 TRPL spectra of STO and STO-OH-5.

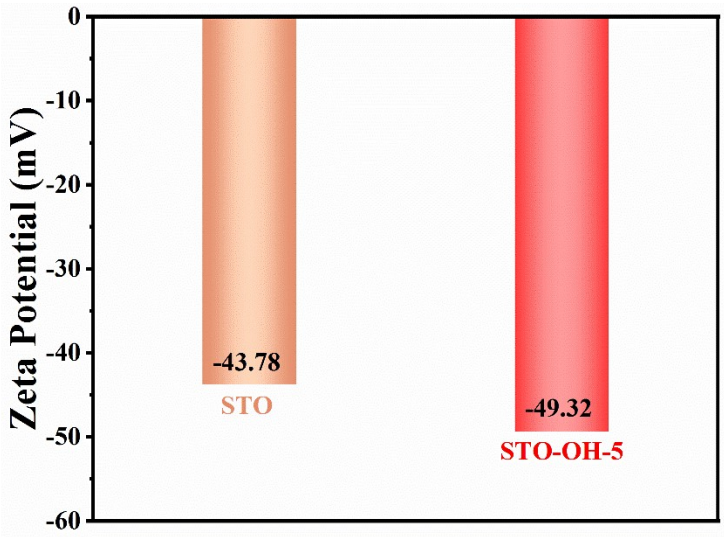

Fig. S10 Zeta potential of STO and STO-OH-5

Table S1. Comparison of photocatalytic activity between STO-OH-5 and recently reported catalysts for CO_2 reduction.

Catalyst	Sacrificial agent	Amount of catalyst	Irradiation condition	CO generation rate	Ref.
STO-OH-5	TEOA	10 mg	300 W Xe lamp	90 μmol/g/h	/
26-facet STO	H_2O	8 mg	300 W Xe lamp	1.77 μmol/g/h	[1]
NH_2-T-COF-TiO_2	ACN Ascorbic acid	10 mg	300 W Xe lamp	1.88 μmol/g/h	[2]
Gd-$ZnIn_2S_4$	TEOA	50 mg	300 W Xe lamp	2.1 μmol/g/h	[3]
CABB@MCM-48	$Ru(bpy)_3^{2+}$ TEOA	20 mg	300 W Xe lamp	10.34 μmol/g/h	[4]
In_2O_3/In_2S_3	H_2O	30 mg	300 W Xe lamp	12.22 μmol/g/h	[5]
BON/CN-2	H_2O	20 mg	300 W Xe lamp	14.84 μmol/g/h	[6]
Ag-Bi_2WO_6	H_2O	20 mg	300 W Xe lamp	19.45 μmol/g/h	[7]
$W_{18}O_{49}$@Co	TEOA	10 mg	300 W Xe lamp	21.18 μmol/g/h	[8]
GACN-2	TEOA ACN	10 mg	300 W Xe lamp	36.79 μmol/g/h	[9]
TiO_2/CdS	$[Ru(bpy)_3]Cl_2 \cdot 6H_2O$ TEOA	10 mg	300 W Xe lamp	47.67 μmol/g/h	[10]
NNO-C1%	$Ru(bpy)_3^{2+}$ Ascorbic acid	15 mg	300 W Xe lamp	49.08 μmol/g/h	[11]
Vo-R-Pd/CeO_2	TEOA	2 mg	300 W Xe lamp	77.9 μmol/g/h	[12]

References

[1] Q.-Q. Shen, W.-X. Kang, L. Ma, Z. Sun, B.-B. Jin, H.-M. Li, Y. Miao, H.-S. Jia and J.-B. Xue, Tuning the anisotropic facet of $SrTiO_3$ to promote spatial charge separation for enhancing photocatalytic CO_2 reduction properties, *Chem. Eng. J.*, 2023, **478**, 147338.

[2] Y. Wang, Z. Hu, W. Wang, Y. Li, H. He, L. Deng, Y. Zhang, J. Huang, N. Zhao, G. Yu and Y. Liu, Rational design of defect metal oxide/covalent organic frameworks Z-scheme heterojunction for photoreduction CO_2 to CO, *Appl. Catal. B-Environ.*, 2023, **327**, 122419.

[3] F.-H. Zhou, Y.-L. Zhang, J. Wu, W. Yang, X. Fang, T. Jia, Y. Ling, P. He, Q.-Z. Liu and J. Lin, Utilizing Er-doped $ZnIn_2S_4$ for efficient photocatalytic CO_2 conversion, *Appl. Catal. B Environ.*, 2024, **314**, 123347.

[4] Z. Zhang, D. Li, Z. Dong, Y. Jiang, X. Li, Y. Chu and J. Xu, Lead-free $Cs_2AgBiBr_6$ nanocrystals confined in MCM-48 mesoporous molecular sieve for efficient photocatalytic CO_2 reduction, *Sol. RRL.*, 2023, **7**, 2300038.

[5] J.-M. Yang, X.-W. Zhu, Q. Yu, M.-Q. He, W. Zhang, Z. Mo, J.-J. Yuan, Y.-B. She, H. Xu and H.-M. Li, Multidimensional In_2O_3/In_2S_3 heterojunction with lattice distortion for CO_2 photoconversion, *Chinese J. Catal.*, 2022, **43**, 1286-1294.

[6] T.-Y. Liu, L. Hao, L.-Q. Bai, J.-G. Liu, Y.-H. Zhang, N. Tian and H.-W. Huang, Z-scheme junction $Bi_2O_2(NO_3)(OH)$/g-$C_3N_4$for promoting CO_2 photoreduction, *Chem. Eng. J.*, 2022, **429**, 132268.

[7] L.-L. Zhao, H.-L. Hou, L. Wang, C.-R. Bowen, J.-G. Wang, R.-F. Yan, X.-Q. Zhan, H.-L. Yang, M. Yang and W.-Y. Yang, Atomic-level surface modification of ultrathin Bi_2WO_6 nanosheets for boosting photocatalytic CO_2 reduction, *Chem. Eng. J.*, 2024, **480**, 148033.

[8] H. Zhang, Y. Wang, S. Zuo, W. Zhou, J. Zhang and X. Lou, Isolated cobalt centers on $W_{18}O_{49}$ nanowires perform as a reaction switch for efficient CO_2 photoreduction, *J. Am. Chem. Soc.*, 2021, **143**, 2173-2177.

[9] Q. Liu, X. Wang, X. Zhu, P. Ding, K. Zhong, J. Liu, Y. Hua, Q. Hu, J. Yi, H. Xu, X. Wang and J. Ding, Unraveling the unique role of brown graphitic carbon nitride in robust CO_2 photoreduction, *Appl. Surf. Sci.*, 2023, **615**, 156173.

[10] Z.-H. Chen, D.-P. Li and C.-J. Chen, Urchin-like TiO_2/CdS nanoparticles forming an S-scheme heterojunction for photocatalytic hydrogen production and CO_2 reduction, *ACS Appl. Nano Mater.*, 2023, **6**, 21897-21908.

[11] X.-F. Wang, J.-W. Jiang, L. Yang, Q. An, Q.-J. Xu, Y.-X. Yang and H. Guo, Enhanced piezoelectric polarization by subtle structure distortion to trigger efficient photocatalytic CO_2RR, *Appl. Catal. B-Environ.*, 2024, **340**, 123177.

[12] F.-L. Kong, X.-Y. Lu, J. Xie, Z.-J. Lu, J.-D. Hu and Y.-L. Cao, Enhanced photocatalytic CO_2 reduction by controlled oxygen vacancy generation and co-constructed heterojunction strategy for Pd/CeO_2, *Inorg. Chem. Front.*, 2024, **11**, 2932-2944.